CHEMISTRY OF MATERIALS
Article

Chem. Mater. **2010,** *22,* 4555–4562 4555
DOI:10.1021/cm100823d

Enzyme-Based Hybrid Macroporous Foams as Highly Efficient Biocatalysts Obtained through Integrative Chemistry

N. Brun,[†,‡] A. Babeau Garcia,[†] H. Deleuze,[‡] M.-F. Achard,[†] C. Sanchez,[§] F. Durand,[†] V. Oestreicher,[†] and R. Backov*[,†]

[†]*Centre de Recherche Paul Pascal, UPR 8641-CNRS, Université Bordeaux 1, 115 Avenue Albert Schweitzer, 33600 Pessac, France,* [‡]*Université Bordeaux I/CNRS, Institut des Sciences Moléculaires* (*ISM*)*, 351 Cours de la Libération, F 33405 Talence, France, and* [§]*Laboratoire Chimie de la Matière Condensée de Paris* (*LCMCP*) *UMR-7574 UPMC−CNRS, Collège de France, 11, place Marcelin Berthelot, 75231 Paris Cedex 05, France*

Received March 23, 2010. Revised Manuscript Received July 16, 2010

Integrative chemistry-based rational design has been used to synthesize the first lipase [C-*CR*l]@Glymo-Si(HIPE) and [C-*TA*l]@Glymo-Si(HIPE) hybrid macrocellular biocatalysts, where immobilization of crude enzymes is optimized, while circumventing the reactants' low kinetic diffusion, by the use of silica macroporous hosts. As a direct consequence, these new hybrid biocatalysts display unprecedented cycling catalysis performance, as demonstrated by the syntheses of butyloleate ester (used as biodiesel lubricant), hydrolysis of linoleic-glycero ester derivatives (end products used for detergent and soap generations), and trans-esterification (reaction involved in the synthesis of low viscosity biodiesel). Considering that the catalytic performances are given in terms of absolute conversion percentage and not just relative enzyme activity, the enzyme@Glymo-Si(HIPE) hybrid macrocellular biocatalysts presented in this study display unprecedented high yield cycling catalysis performances, where turnover numbers (TON) and turnover frequencies (TOF) show promise for real industrial applications. This study can be considered as a milestone for enzyme-based heterogeneous catalyzes, thereby enhancing their competitiveness with the supported-catalysts commonly used in industry, in total agreement with current sustainable development issues. Also, the new macrocellular biocatalysts are well-suited for large-scale industrial production because of their above-mentioned performance characteristics, further enhanced by their monolithic character, which eases the separation of the catalysts from other reaction components.

Introduction

With the emergence of the green chemistry criteria,[1] modern chemical science research efforts, both academic and industrial, are strongly directed toward novel synthetic pathways, which decrease the use of solvents, are safe for the environment, use bioresources as precursors, and have some degree of reusability, thereby achieving the notion of sustainable development. Simultaneously, chemists are requested to envisage materials that are increasingly complex in nature and structure, have more than one functionality, and at the extreme are inspired by living organisms. To construct such highly advanced functional materials, chemical science cannot be restricted to a single specific domain of chemistry. Rather, a strong interdisciplinary approach is needed, crossing chemical boundaries and beyond. In such a context, there is a crucial need for "rational design" of functional architectures, in which the primary concern is not only the "chemistry of shapes" or even the competence and methodology in use, but rather the enhanced function or intended use, which will ultimately determine the best overall synthetic pathway. From this way of thinking has recently emerged the concept of integrative chemistry,[2,3] which is applied herein to the design of highly efficient porous enzyme-based supported catalysts.

In chemistry, heterogeneous catalysis is certainly the area where the strongest efforts are needed, because catalyzed reactions are involved both in decontamination processes and in synthesis of compounds dedicated either to the pharmaceutical or petroleum industries. In this regard, enzyme-based heterogeneous catalysts are considered as potentially outstanding candidates, but to date enzyme immobilization/activation has been associated with slow kinetics due to low diffusion rates. Coupled with the high cost of these materials, their use on the industrial scale has been severely restricted. To design high-performing heterogeneous biocatalysts, all the key parameters that determine the final activity must be balanced. The reactive surface and catalyst accessibility

*Corresponding author. E-mail: backov@crpp-bordeaux.cnrs.fr.

(1) Anastas, P. T.; Warner, J. C. *Green Chemistry Theory and Practice*; Oxford University Press: New York, 1998.
(2) Backov, R. *Soft Matter* **2006**, *2*, 452.
(3) Prouzet, E.; Ravaine, S.; Sanchez, C.; Backov, R. *New J. Chem.* **2008**, *32*, 1284.

Published on Web 07/30/2010

Scheme 1. Structure of the Two Enzymes in Use in This Study: (a) *Candida Rugosa* Lipase (*CR*l), pdb-1crl,[18] and (b) *Thermomyces lanuginosus* Lipase (*TL*l), pdb-1dt3[19]

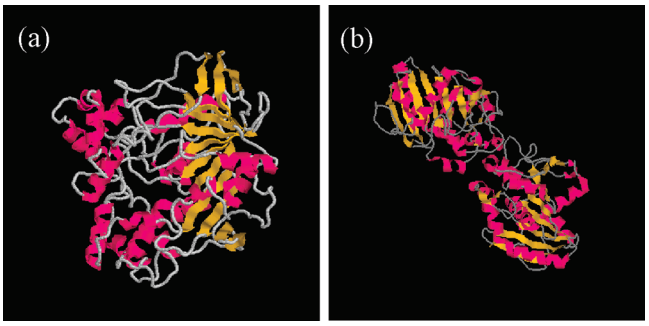

and stability must be optimized, while avoiding, as far as possible, problems with slow diffusion.[4] At this stage, these are competitive goals, because design of high-performance enzyme-based catalyst supports to improve enzyme stability via confinement is not commensurate with good accessibility. These features, along with the relatively high cost of enzymes, are certainly the reasons why biocatalyst industrial applications have not yet reached a significant level.

Among heterogeneous catalysis strategies, immobilization, and encapsulation of enzymes either within inorganic solids,[4,5] sol−gel derived matrices,[6−9] or membranes[10] have been active research areas because of the great potential for use as biocatalysts[11] and biosensors,[12] and also because these enzyme-based hybrid functional materials intrinsically promote the use of biomass components. Lipases (triacylglycerol acyl hydrolases, EC. 3.1.1.3) are ubiquitous enzymes with various biological functions, including enantioselective hydrolysis and esterification,[13] chiral resolution,[14] synthesis of enantiomeric monomers and macromolecules for polymerization reactions,[15] etc. Among the lipases from various sources, *Candida rugosa* lipase (*CR*l) has received much attention because of its high activity and specificity for a range of substrates,[16] whereas *Thermomyces lanuginosus* lipase (*TL*l) appears as an outstanding candidate for transesterification catalysis reactions involved in biodiesel production.[17] Both structures are proposed within Scheme 1. In this study, these two lipase enzymes will be used as reactive guests stabilized by silica-hybrid meso-macrocellular monolith hosts.

Lipases have very complex catalytic mechanisms. In aqueous homogeneous solution, lipases are in equilibrium between two conformational states:[20,21] a "closed" inactive form, in which the catalytic triad (aspartate, histidine, and serine) in the active site is covered by a helical "lid" (flap), and an "open" (active) form, in which the lid has been displaced, adopting a totally different conformation and exposing the catalytic residues. This lid opening leads to the formation of a short-lived acyl-enzyme intermediate, which reacts with water or alcohol to produce the acids or the esters, respectively. In particular, when hydrophobic substrates interact with the lipase, the lid opens and thus exposes the active site by a process known as "facial activation".[22] The control of the hydrophobic−hydrophilic balance of matrices has been a way to optimize enzymatic efficiency.[8,9]

Currently, one area of research has been directed to optimization of catalytic reactions in organic media, because all pharmaceutical or bio fuel end products are insoluble in water. Also, it is known that water molecules act as enzyme lubricants,[25,25] and that enzymes can also work in organic solvents containing little or even no water.[26,27] Immobilization/activation of enzymes is then the key to expanding the applications of these natural catalysts, thereby leading to easy separation and purification of the end products from reaction mixtures, efficient recovery of the enzyme-based catalyst, versatility regarding the hydrous/anhydrous character of the solvent in use, and minimization as far as possible of slow diffusion that occurs because of enzyme confinement.

Experimental Section

Materials. Tetraethyl-orthosilane (TEOS), tetradecyltrimethylammonium bromide (TTAB), (3-Glycidyloxypropyl)trimethoxysilane, and dodecane were purchased from Fluka. Lipase from *Candida rugosa* (E.C.3.1.1.3, Type VII, 700 U/mg) and lipase from *Thermomyces lanuginosus* (solution, ≥100 000 U/g) were purchased from Sigma Chemical (St. Louis, MO). Oleic acid, glyceryl trilinoleate (98%), ethyl linoleate (≥99%), linoleic acid (≥99%), n-heptane, ethanol, and 1-butanol were purchased from Sigma and

(4) Mahmood, I.; Guo, C.; Xia, H.; Ma, J.; Jiang, Y.; Liu, H. *Ind. Eng. Chem. Res.* **2008**, *47*, 6379.
(5) Kang, Y.; He, J.; Guo, X.; Song, Z. *Ind. Eng. Chem. Res.* **2007**, *46*, 4474.
(6) Audebert, P.; Demaille, C.; Sanchez, C. *Chem. Mater.* **1993**, *5*, 911.
(7) Avnir, D.; Braun, S.; Lev, O.; Ottolenghi, M. *Chem. Mater.* **1994**, *6*, 1605.
(8) Reetz, M. T.; Zonta, A.; Simpelkamp, J.; Könen, W. *Chem. Commun.* **1996**, 1396.
(9) Reetz, M. T.; Zonta, A.; Simpelkamp, J. *Angew. Chem., Int. Ed.* **1995**, *34*, 301.
(10) Li, N.; Sabakie, K. *J. Membr. Sci.* **2008**, *314*, 183.
(11) Dzige, N.; Aydiner, C.; Imer, D. A.; Bayramoglu, M.; Tanriseven, A.; Keskinler, B. *Bioresour. Technol.* **2009**, *100*, 1983.
(12) Chung, K. E.; Lan, E. H.; Davidson, M. S.; Dunn, B. S.; Valentine, J. S.; Zinc, J. I. *Anal. Chem.* **1995**, *67*, 1505.
(13) Ong, A. L.; Kamarruddin, A. H.; Bhatia, S.; Long, W. S.; Lim, S. T.; Kumari, T. *Enzyme Microb. Technol.* **2006**, *39*, 924.
(14) Ghanen, A.; Enein, H. Y. A. *Tetrahedron: Asymmetry* **2004**, *15*, 3331.
(15) Karla, B.; Kumar, A.; Gross, R. *Chem. Rev.* **2001**, *1001*, 2097.
(16) María, P. D.; Montero, J. M. S.; Sinisterra, J. V.; Alcántara, A. R. *Biotechnol. Adv.* **2006**, *24*, 180.
(17) Dizge, N.; Aydiner, C.; Imer, D. Y.; Bayramoglu, M.; Tanriseven, A.; Keskinler, B. *Bioresour. Technol.* **2009**, *100*, 1983.
(18) Grochulski, P.; Li, Y.; Schrag, J. D.; Bouthillier, F.; Smith, P.; Harrison, D.; Rubin, B.; Cygler, M. *J. Biol. Chem.* **1993**, *268*, 12843.
(19) Brzozowski, A. M.; Savage, H.; Verma, C. S.; Turkenburg, J. P.; Lawson, D. M.; Svendsen, A.; Patkar, S. *Biochemistry* **2000**, *39*, 15071.
(20) Van Tilbeurgh, H.; Sarda, L.; Verger, R.; Cambillau, C. *Nature* **1992**, *369*, 159.
(21) Van Tilbeurgh, H.; Egloff, M.-P.; Matinez, C.; Rugani, N.; Verger, R.; Cambillau, C. *Nature* **1993**, *362*, 814.
(22) Brzozowski, A. M.; Derewenda, U.; Derewenda, Z. S.; Dodson, G. G.; Lawson, D. M.; Turkenburg, J. P.; Bjorkling, F.; Huge-Jensen, B.; Patkar, S. A.; Thim, L. *Nature* **1991**, *351*, 491.
(23) Okahata, Y.; Mori, T. *Trends Biotechnol.* **1997**, *15*, 50.
(24) Kuntz, I. D.; Kauzmann, W. *Adv. Protein Chem.* **1974**, *28*, 239.
(25) Rupley, J. A.; Careri, G. *Adv. Protein Chem.* **1991**, *41*, 37.
(26) Klibanov, A. M. *Nature* **2001**, *409*, 241.
(27) Koskinen, A. M.; Klibanov, A. M. *Enzymatic Reactions in Organic Media*; Blackie-Pergamon: London, 1996.

Aldrich (Paris, France). Other chemicals and solvents used in this study were of analytical grade or HPLC grade.

Synthetic Pathways. *Syntheses of Native Silicon High Internal Phase Emulsion Si-(HIPE).* TEOS (5.02 g) was added to an aqueous solution of tetradecyltrimethylammonium bromide (TTAB) (16.02 g). Then, concentrated hydrochloric acid solution (37%) was added (5.88 g). The aqueous phase was allowed to stir for approximately 5 min for the TEOS to hydrolyze. Then the emulsion was ground in a mortar with dropwise addition of dodecane (40.05 g). The emulsion was transferred to a plastic flask and left to age for 3 days at room temperature. The resulting material was washed with THF, dried in air, and cured at 650 °C for 6 h (heating rate of 2 °C/min with a first plateau at 200 °C for 2 h).

Synthesis of Grafted Glymo-Si(HIPE) Supports. A one-gram piece of native Si-(HIPE was added to a solution of (3-Glycidyloxypropyl)trimethoxysilane organosilane (Glymo) (0.01 mol) in chloroform (120 g). The suspension was placed under vacuum to enhance impregnation. After 48 h at room temperature, the solution was filtrated, and the monoliths were then washed with chloroform and acetone and dried in air.

Lipase Immobilization. Crude lipase from *Candida rugosa* (540 mg) was dispersed in distilled water (18 mL). The mixture was first stirred for an hour. The immobilization of lipase was carried out by introducing the Glymo-Si(HIPE) open cell monolith (250 mg) into the enzyme solution, and a vacuum (20 mbar) was applied for 72 h at ambient temperature. Crude lipase from *Thermomyces lanuginosus* (53 mg) was dissolved in distilled water (10 mL). The Glymo-Si(HIPE) (350 mg) was added to the enzyme solution, and a vacuum (20mbar) was applied for 72 h at ambient temperature. The immobilized lipases were then extracted from the impregnation media and washed three times with distilled water in order to remove the excess enzyme. The final [C-*CR*l]@Glymo-Si(HIPE) and [C-*TL*l]@Glymo-Si(HIPE) heterogeneous catalysts are then dried at room temperature for 12 h and stored in a refrigerator at 4 °C. The stoichiometries of the *Candida rugosa* and *Thermomyces lanuginosus*-based heterogeneous catalysts were determined by combined C,H,N elemental analysis data and TGA experiments.

Set-up of the Catalytic Reactions. *Esterification Catalysis Reactions.* The enzymatic esterification reaction consisted of 1-butanol (2.0×10^{-3} mol), oleic acid (1.0×10^{-3} mol), a piece of monolith [C-*CR*l]@Glymo-Si(HIPE) (247 mg) and heptane (2 mL). The reaction mixture was incubated at 37 °C for 24 h under gentle stirring to avoid breaking the monoliths. Formation of the ester was monitored using HPLC to determine the conversion rate.

Homogeneous catalysis with free lipases was carried out in heptane (2 mL), with 1-butanol (2.0×10^{-3} mol), oleic acid (1.0×10^{-3} mol), and crude *Candida rugosa* lipase (17.5 mg). The reaction was incubated at 37 °C for 40 h with vigorous stirring. Formation of ester was monitored using HPLC to determine the conversion rate.

Triester Hydrolysis Catalysis Reactions. In this experiment, a 200 mg piece of monolith, [C-*CR*l]@Glymo-Si(HIPE), was placed into 15 mL of water-saturated heptane. After reaching the desired temperature between 37 and 38 °C, 100 μL of a glyceryl trilinoleate (triester) dissolved in methyl-*tert*-butyl ether (MTBE) was addedat a concentration of 100 mg/mL, leading finally to a triester solution with a concentration of 0.66 mg/mL. The catalysis batch process was performed with slow stirring. HPLC was used to check the disappearance of reagent and appearance of both the final product and intermediates. After 24 h of catalytic cycling, and prior to performing a new catalytic run, the monolith was extracted from the vessel and washed three times with the water-saturated heptane solution.

Trans-Esterification Catalysis Reactions. Reactions were performed as batch processes in 4 mL of heptane in glass tubes containing 100 μL of glyceryl trilinoleate previously dissolved in methyl tert-butyl ether at a concentration of 100 mg/mL, 25 mg of ethanol and a 387 mg piece of monolith [C-*TL*l]@Glymo-Si(HIPE). The reaction mixture was incubated at 37 °C for 24 h with slow stirring. Conversion of glyceryl trilinoleate was monitored using HPLC.

Characterizations. Scanning electron microscopy (SEM) observations were performed with a Jeol JSM-840A scanning electron microscope operated at 10 kV. Intrusion/extrusion mercury measurements were performed using a Micromeritics Autopore IV apparatus in order to assess the scaffolds' macrocellular cell characteristics. Surface areas and pore characteristics at the mesoscale were obtained by nitrogen adsorption−desorption experiments using a Micromeritics ASAP 2010. Small-angle X-ray scattering (SAXS) experiments were carried out on an 18 kW rotating-anode X-ray source (Rigaku-200) using a Ge (111) crystal as monochromator. The scattered radiation was collected on a two-dimensional detector (Imaging Plate system from Mar Research, Hamburg). The sample- detector distance was 500 mm. TEM was performed using a HITACHI − H7650 TEM operated at 80 kV equipped with an ORIUS GATAN (11MPX) camera.

HPLC Analytical System. The analytical system consisted of a model 600 solvent delivery system with a manual injector (Waters, Milford, MA). The compounds were separated on an Atlantis DC_{18} (4.6 mm × 150 mm, 5 μm) column with an Atlantis DC_{18} guard column (Waters) using an isochratic mobile phase of HPLC-grade acetonitrile. The column was operated at room temperature. EMPOWER software (Waters) was used for data acquisition and processing. Standards were dissolved in methyl *tert*-butyl ether (MTBE). All solutions were filtered through a 0.45 μm membrane and degassed before use. The mobile phase flow-rate was 1 mL/min and 20 μL samples were injected. A model 410 refractometer (Waters, Milford, MA, USA) was used for detection of the esterification reaction. For both the hydrolysis and trans-esterification reactions the detector was an ultraviolet diode array 996 (Waters, Milford, MA). The absorbance maximum was at λ = 204 nm. A gradient elution was used: solvent A, acetonitrile; solvent B, methyl *tert*-butyl ether; 4 min isochratic at 100% (v/v) A; 2 min gradient to 70/30 (v/v) A/B; isocratic for 10 min at 70/30 (v/v) A/B; 0.5 min return to 100% (v/v) A; 10 min re-equilibration with 100% A.

Results and Discussion

Synthesis and Characterization of Biocatalyst Foams. In the present study, the confinement media were organo-silica-based hybrid macrocellular monolithic foams having hierarchical porous structures. The monolith-type material observed in Figure 1a was obtained through a double template process making use of direct emulsion to create the macroporosity and a lyotropic mesophase both to stabilize the oil/water interface and to create micellar-induced mesoscopic porosity.[28] The macroscopic cell sizes of such architectures vary depending on the initial oil volume fraction. We labeled this new series of materials "Si(HIPE)" with the acronym HIPE for "high internal phase emulsion".[29]

(28) Carn, F.; Colin, A.; Achard, M.-F.; Birot, M.; Deleuze, H.; Backov, R. *J. Mater. Chem.* **2004**, *14*, 1370.
(29) Cameron, N. R.; Sherrington, D. C. *Adv. Polym. Sci.* **1996**, *126*, 162.

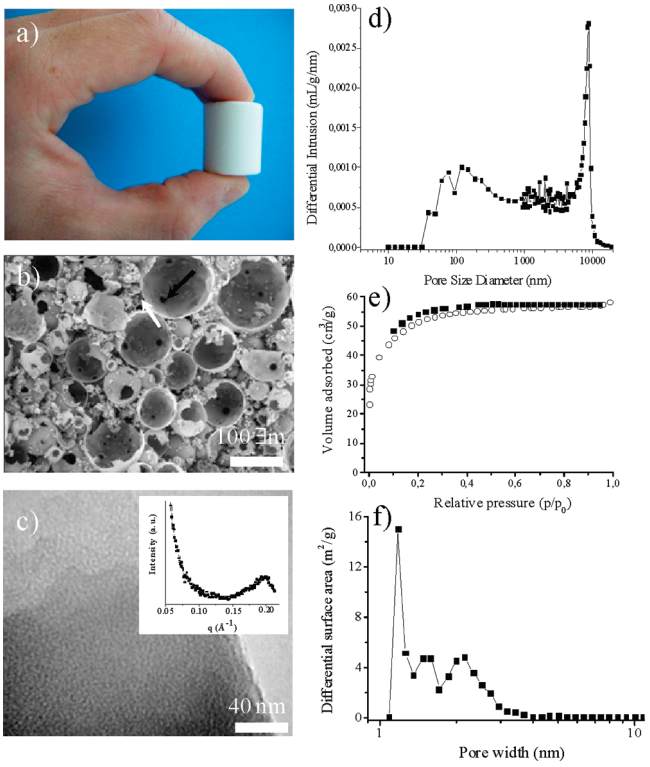

Figure 1. Examples of support textural characteristics at three length scales of the as-synthesized Enzyme(*CRl*)@Glymo-Si(HIPE) macrocellular foam: (a) Photograph of the as-synthesized monoliths, (b) SEM micrograph where the black arrow indicates an internal junction while the white arrow indicates an external junction, (c) TEM pictures depicting mesoporous void spaces (SAXS profile, embedded), (d) size distribution of the macroscopic pore openings, (e) nitrogen adsorption (○)−desorption (■) measurements, (f) resulting distribution of the mesoscopic pore sizes (obtained by the density functional theory). The full surface characterization for all hybrid foams in use, both at the macroscopic and mesoscopic length scales, can be found in the Supporting Information.

Recently, we developed a new generation of hybrid Organo-Si(HIPE)[30] series having organic functionalities, such as mercapto, diamino, benzyl, dinitro, etc., derivatives at the molecular level. These allow the functionalities of the final porous materials to be directed toward either heterogeneous catalysis[31] or photoluminescence.[32] The present study is the first use of (3-Glycidyloxypropyl)trimethoxysilane (Glymo) as a functional agent to stabilize the embedded enzymes. This methodology allows preparation of net-shaped monolithic materials that can be easily manipulated, separated and transferred (Figure 1a). As shown in Figure 1b, the texture resembles an aggregate of hollow spheres because of the pH-induced Euclidian character[29,33] of the inorganic walls. As a direct consequence, two kinds of pore openings connecting adjacent cells must be considered: the intrawall pore openings (previously called internal junctions) and the pore openings from the hollow sphere aggregation (previously called external junctions).[29]

The distribution of the interconnected pore opening sizes, as measured by mercury intrusion porosimetry (Figure 1d), covers a broad range (50 to 5000 μm) with a major contribution at 9000 μm. Specific morphological characterizations were 94% porosity, 0.085 g/cm^{-3} bulk density, and 1.56 g/cm^{-3} skeleton density. It is noteworthy that these monolithic materials have the same bulk density as common silica aerogel[34] and can endure the mercury impregnation process, thus indicating good mechanical properties. At the mesoscopic length scale, these hybrid foams have vermicular-type mesopores associated with a wall-to-wall average distance of 31 Å, as shown in Figure 1c. Nevertheless, when considering the nitrogen physisorption (Figure 1e,f) measurements, which strongly suggest a relatively high microporosity (BET = 170 m^2 g^{-1}) and low mesoporosity (BJH = 45 m^2 g^{-1}), there is at first glance a certain collapse of mesoporosity when compared with pure inorganic Si(HIPE) foams.[28] In fact, it is very well established that postgrafting of silane tends to strongly block the mesoporous nodes, minimizing nitrogen accessibility to the interior of the mesopores.[35−38]This feature is certainly enhanced here because of the enzyme adjunction. As a direct consequence, all subsequent catalyzed reactions will occur exclusively inside the macropores. The full surface characterization both at the macroscopic and mesoscopic length scales can be found in the Supporting Information.

Also at the microscopic length scale, it is important to provide stoichiometries of the as-synthesized biocatalysts, in order to both relate and normalize catalytic performances with enzyme activity. The stoichiometries of the *Candida rugosa* and *Thermomyces lanuginosus* based heterogeneous catalysts were obtained through combined C, H, N elemental analysis and thermal gravimetric analysis (TGA) and are, respectively, $[C.\ CR1]_{9.10}{}^{-5}@Si_{1.91}(C_6O_2H_{11})_{0.09}\cdot 0.09H_2O$ and $[C\text{-}TLl]_{8.10}{}^{-5}@SiO_{1.95}(C_6O_2H_{11})_{0.05}\cdot 0.06\ H_2O$. The crude *Candida rugosa* lipase had a purity of 3 wt %, whereas the crude *Thermomyces lanuginosus* had a purity of 95 wt % (see the Supporting Information for the employed Bradford purification technique). Quantitatively, there was 2.3 mg of active enzyme per gram of catalyst for [C-*CRl*]@Glymo-Si(HIPE) and 31 mg of active enzyme per gram of catalyst for [C-*TLl*]@Glymo-Si(HIPE). Also the grafting of the Glymo moieties through condensation was verified by ^{29}Si NMR spectroscopy (see the Supporting Information).

Catalytic Activity of the Enzyme Biocatalyst Foams. Three main reactions were chosen to test these enzyme-based heterogeneous catalysts: a simple esterification reaction, a reaction based on triester hydrolysis, and a trans-esterification reaction associated with biodiesel production. All the above-mentioned reactions can be found in Scheme 2.

(30) Ungureanu, S.; Birot, M.; Guillaumme, L.; Deleuze, H.; Babot, O.; Julian, B.; Achard, M.-F.; Popa, M. I.; Sanchez, C.; Backov, R. *Chem. Mater.* **2007**, *19*, 5786.
(31) Ungureanu, S.; Deleuze, H.; Popa, M. I.; Sanchez, C.; Backov, R. *Chem. Mater.* **2008**, *20*, 6494.
(32) Brun, N.; Julian-Lopez, B.; Hesemann, P.; Guillaume, L.; Achard, M.-F.; Deleuze, H.; Sanchez, C.; Backov, R. *Chem. Mater.* **2008**, *20*, 7117.
(33) Brinker, C. J.; Scherer, G. W. *Sol−Gel Science: The Physics and Chemistry of Sol−Gel Processing*; Academic Press: London, 1990.
(34) Hüsing, N.; Schubert, U. *Angew. Chem., Int. Ed.* **1998**, *37*, 22.
(35) Moller, K.; Bein, T. *Chem. Mater.* **1998**, *10*, 2950.
(36) Stein, A.; Melde, B. J.; Schroden, R. C. *Adv. Mater.* **2000**, *12*, 1403.
(37) Nicole, L.; Boissière, C.; Grosso, D.; Quach, A.; Sanchez, C. *J. Mater. Chem.* **2005**, *15*, 3598.
(38) Hoffmann, F.; Cornelius, M.; Morel, J.; Fröba, M. *Angew. Chem., Int. Ed.* **2006**, *45*, 3216.

Scheme 2. Three Typical Reactions Chosen for Testing the As-Synthesized Enzyme-Based Catalyst Performances: Top, Esterification of Oleic Acid (1) with Butanol (2) Providing Butyl Oleate Ester (3); Middle, Hydrolysis of Trilinolein (4) Providing Linoleic Acid (5) and Glycerol (6) (Intermediate Products (4′) 1,3-Dilinolein, (4″) 1,2-Dilinolein, (4‴) 1-Monolinoleoyl-*rac*-glycerol); Bottom: Trans-Esterification of Trilinolein (4) with Ethanol (7) Providing Glycerol (6) and Ethyl Linoleate Ester (8)

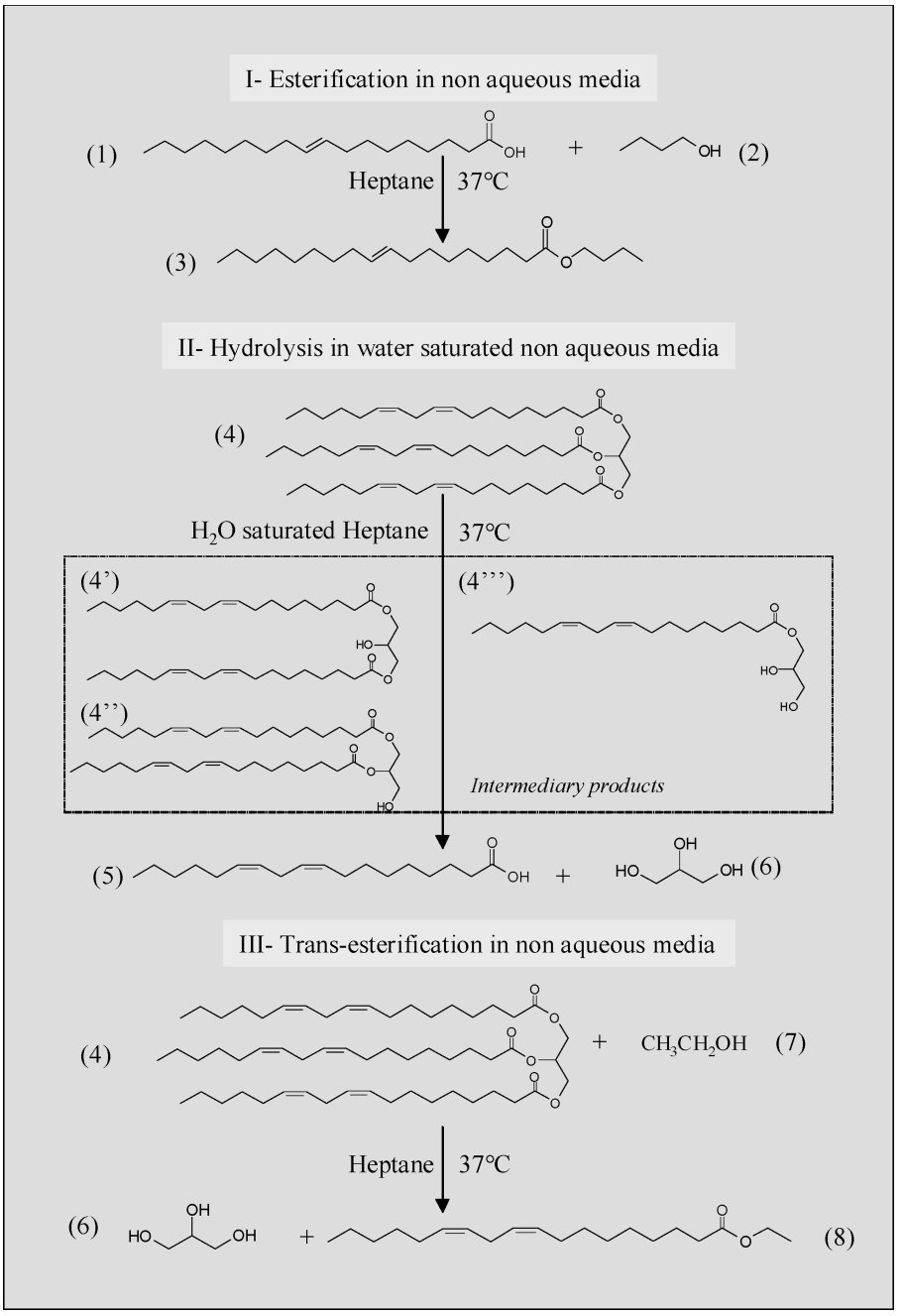

Enzyme-Based Heterogeneous Catalysis of Esterification Reactions. The first chemical reaction chosen to evaluate the as-synthesized enzyme-based catalyst performance was the well-known esterification of oleic acid with butanol to provide butyl-oleate ester (Scheme 2), this ester being an essential biodiesel additive acting as lubricant during winter use.[39] To assess enzyme heterogeneous catalysis, it is also important to consider enzyme homogeneous catalysis, in order to appreciate the host confinement effect. This first experiment is addressed in Figure 2.

Figure 2a shows that the conversion kinetics are greatly enhanced by heterogeneous catalysis compared to the homogeneous system. The conversion rate (Figure 2b) for homogeneous conversion rate is 0.9 μmol min^{-1} mg^{-1}, whereas the initial rate of the heterogeneous reaction is 23.5 μmol min^{-1} mg^{-1}. This result demonstrates without ambiguity the enhancement of enzyme activity via confinement; in the case of Glymo-Si(HIPE) confinement, the enzymatic activity for this esterification reaction is increased by about 25-fold. Also the conversion by homogeneous catalysis was not completed after 24 h, but the heterogeneous system led to 100% conversion

(39) Linko, Y.-Y.; Lämä, M.; Wu, X.; Uosukainen, E.; Seppälä, J.; Linko, P. *J. Biotechnologies* **1998**, *66*, 41.

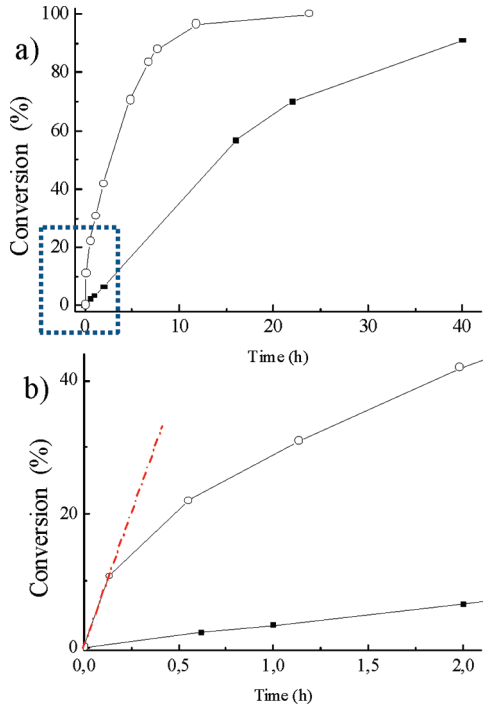

Figure 2. Enzymatic catalytic performance in an esterification reaction. (a) ○ [C-CRl]@Glymo-Si(HIPE) heterogeneous catalysis; ■ [C-CRl] homogeneous catalysis (17.5 mg of commercial *Candida rugosa* crude Lipase in heptane). (b) Zoom of the blue dashed area of a: ○ [C-CRl]@Glymo-Si(HIPE) heterogeneous catalysis; ■ [C-CRl] homogeneous catalysis (17.5 mg of commercial *Candida rugosa* crude Lipase in heptane). The red dashed line corresponds to the slope of the conversion versus time for the first 10 min of reaction.

after about 12 h. The results in Figure 2 also show that the enzyme concentration within the heterogeneous catalyst was not excessive. This is the first reason why the same catalytic experimental setup was chosen to evaluate the cycling performance of the [C-*CR*l]@Glymo-Si(HIPE) heterogeneous catalysts. Another reason is that this experimental setup is nearly the same as that for the best enzyme-based heterogeneous catalysts found in the literarure.[40−43]

As shown in Figure 3, the [C-*CR*l]@Glymo-Si(HIPE) catalyst was able to cycle for 19 runs with 100% of conversion in each cycle. There was a small decrease in the catalytic activity for the 20th and 21st runs, in agreement with the observation of partial collapse of the monolith and consequent loss of enzyme into the reaction batch. Despite final catalyst collapse it may be argued that the conversion reached 100% for 19 runs because the amount of active enzyme was very high (or oleic acid concentration was very low). However, the oleic acid and active enzyme concentrations were exactly the same as those used for the homogeneous catalysis, which did not achieve complete conversion even after 24 h (Figure 2).

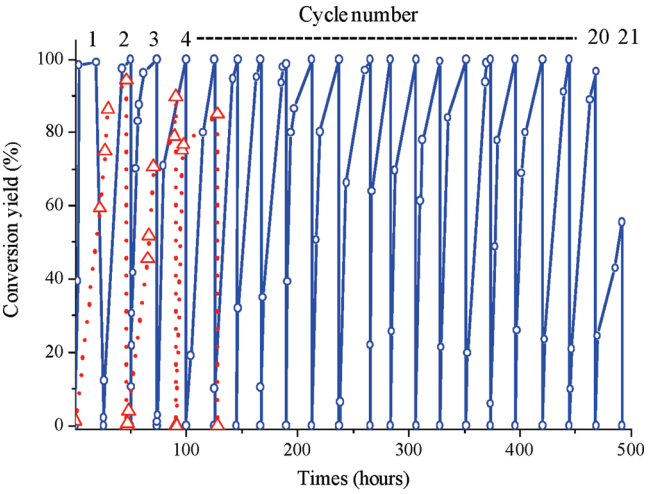

Figure 3. *Candida rugosa*-based heterogeneous catalyst performance. [C-*CR*l]@Glymo-Si(HIPE)-based esterification reactions: ○, Glymo stabilized enzyme; △, without Glymo.

Thus, the results obtained for the heterogeneous catalysis are due to the intrinsic biohybrid catalyst performance. Also, when performing these cycles, the [C-*CR*l]@Glymo-Si(HIPE) was stored at 4 °C for 2 months between cycles 10 and 11 and, as shown in Figure 3, without any loss of catalytic activity. Thus, in addition to having high catalytic activities, these enzyme-based catalysts can be stored in a refrigerator at 4 °C without any special precautions.

When compared with the currently best enzyme-based heterogeneous catalysts,[40−43] [C-*CR*l]@Glymo-Si(HIPE) shows significantly enhanced esterification catalytic performance with excellent stability over time. The conversions observed with other supports currently in use, e.g., polyurethane foam,[40] calcium carbonate,[41] silica gel 60,[41] Amberlite IRC-50,[41] Celite 545,[41] natural kaolin,[42] and layered double hydroxides,[43] were always below 85% over at most 9 cycles with lipase life times of 12 days at best. Also, to decrease the cost of this enzyme-based catalyst, we investigated the need for Glymo entities. Catalytic tests with the [C-*CR*l]@Si(HIPE) catalytic support free of the "Glymo" stabilizing agent were performed, and the results are provided in Figure 3 (Δ symbols). The first conversion was around 95% complete with a slower kinetics (double reaction time). With cycling, the conversions decreased to 87% with slower kinetics when compared to the catalyst support having the Glymo entities acting as enzyme stabilizing agents. This result confirms that even with crude enzyme, Glymo molecules, which hydrolyze spontaneously in water to generate diol functional groups, are indeed necessary to improve enzyme stability and hydration and thereby the catalytic activity.[44]

Enzyme-Based Heterogeneous Catalysis of Hydrolysis Reactions. The second reaction chosen to test the [C-*CR*l]@Glymo-Si(HIPE) catalytic activity was triester hydrolysis (Scheme 2), specifically the hydrolysis of a trilinolein ester which, with triglyceride esters of oleic and palmitic acid, represents a major component of olive oil. Moreover, the corresponding linoleic acid and linoleate

(40) Awang, R.; Basri, M. R. G. M. *Am. J. Biochem. Biotechnol.* **2007**, *3*, 163.
(41) Ghamgui, H.; Karra-Chaâbouni, M.; Gargour, Y. *Enzyme Microb. Technol.* **2004**, *35*, 355.
(42) Rahman, M. B. A.; Tajudin, S. M.; Hussein, M. Z.; Rahman, R. N. Z. R. A.; Sallehb, A. B.; Basri, M. *Appl. Clay Sci.* **2005**, *29*, 111.
(43) Rahman, M. B. A.; Basri, M.; Hussein, M. Z.; Idris, M. N. H.; Rahman, R. N. Z. R.; Salleh, A. B. *Catal. Today* **2004**, *93−95*, 405.
(44) Wheatleya, J. B.; Schmidt, D. E. *J. Chromatogr., A* **1999**, *849*, 1.

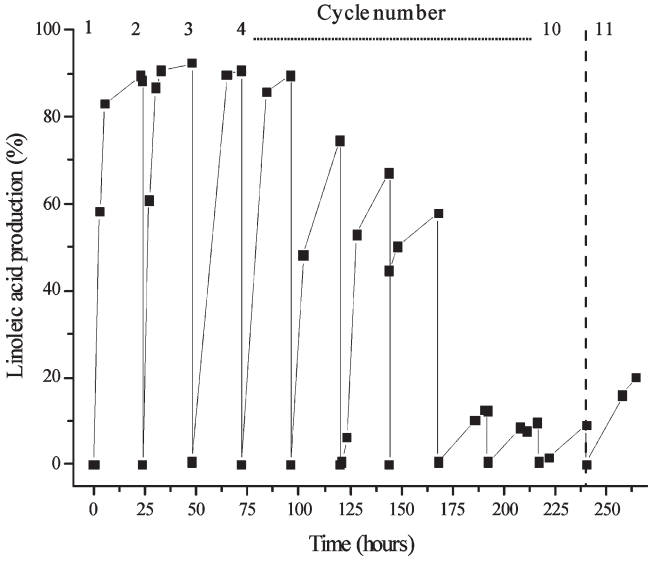

Figure 4. [C-*CR*l]@Glymo-Si(HIPE) linoleic acid production through triester hydrolysis. The dashed line at the beginning of the 11th cycle indicates that catalyst hydration has been performed prior this new cycle.

esters have two double bonds, which are easily by HPLC (see Experimental Section). Usually, enzyme-based catalysts are tested by ester hydrolysis in water of either *p*-nitophenyl palmitate (*p*NPP) or *p*-nitrophenyl acetate (*p*NPA),[45] because the nitrophenyl group can be easily followed by UV−vis experiments, and because water, being the solvent, is not a limiting reagent. Real olive oil triester derivatives are very seldom used because of several issues. First, the triesters are mostly insoluble in water, so that the solution in use for the catalysis can be at best only a "water-saturated" nonaqueous medium. Second, both the triester, the intermediate diesters, and the final oleic acid (Scheme 2) are not easily followed using HPLC. Despite those problems, some successes have been achieved using either polypropylene modified membranes,[46] magnetic microspheres,[47] or layered double hydroxides (LDHs)[48]as supported media.

The results in Figure 4 show that [C-*CR*l]@Glymo-Si(HIPE) keeps producing a conversion of at least 80% for the first four cycles and above 65% for the remaining cycles.

These conversion percentages are higher than those obtained with enzyme stabilized in open structures: polypropylene membranes[46] (loss of around 6% of the initial activity by the fourth cycle) and LDHs[48] (conversion lower than 80% for the first batch and loss of around 10% of the initial activity by the fourth cycle). Moreover, reusability of the [C-*CR*l]@Glymo-Si(HIPE) is as good as that reported for enzyme stabilized with magnetic porous microspheres.[47] We first thought that the decrease of conversion observed in Figure 4 was caused by the inherent protein denaturation and substantial leakage from the support, as claimed elsewhere.[45−47] However, when the catalyst was rehydrated (Figure 4, dashed line), the [C-*CR*l]@Glymo-Si(HIPE) regained the catalytic activity of the enzyme. Water has to be added to ensure the enzyme's structural integrity and catalytic activity.[22−27] This means that the lack of catalyst hydration, even using a water saturated heptane solution (0.6 wt %), is indeed a major problem for the hydrolysis reaction itself. Also, hydrolysis performances reached with the magnetic microsphere[47] bead catalysts were obtained with hydration between 25 and 65 wt % water (around 100 times higher than that of the experiment described here), enhancing the intrinsic hydrolysis reaction, but also certainly leading to a triphasic system, i.e., water in oil biphasic emulsion and the solid-state catalyst itself. This overall scenario appears at first glance to make supported catalyst use difficult on the industrial. This is the reason why we chose to minimize, as far as possible, the water content in the reaction medium when dealing with this biocatalyzed hydrolysis reaction, working thereby in the worst reaction conditions but optimizing the industrial potential applications. The high performance of the [C-*CR*l]@Glymo-Si(HIPE) catalyst, despite functioning with very low amounts of water, is certainly due to the intrinsic hydration of silica (see the catalysts' stoichiometry in the Experimental Section), which favors enzyme stability. This inherent hydration characteristic is also important in the following biocatalyzed reaction.

Enzyme-Based Heterogeneous Catalysis of Trans-Esterification Reactions. The third reaction chosen for testing the enzyme-based biocatalysts was the transesterification reaction mainly involved in biodiesel production (Scheme 2). For this particular catalysis reaction the C. Rugosa has been shown to offer poor efficiency for biodiesel production, whatever the support in use, for instance Celite[49] or kaolite.[50] For this reason, we used *Thermomyces lanuginosus* lipase (Scheme 1) to generate a new [C-*TL*l]@Glymo-Si(HIPE) heterogeneous biocatalyst. This was also a direct way to demonstrate that use of Glymo-Si(HIPE) as the host-support is not restricted to the *C. Rugosa* lipase. In particular, the lipase from *T. Lanuginosus* has demonstrated good efficiency toward biodiesel production, when supported on Celite,[51] acrylic resin,[52] polymeric macroporous foams,[13] and silica-poly (vinyl alcohol) composite.[53] As with *C. Rugosa*, the *T. Lanuginosus* was employed as a crude material for impregnation into the host Glymo-Si(HIPE), leading to the catalyst [C-*TL*l]@Glymo-Si(HIPE). Figure 5 shows that that the first cycle achieved 100% conversion within 24 h at 37 °C.

This result is much higher than the conversions obtained previously for *T. Lanuginosus lipase* as guest for heterogeneous catalysts.[17,52,53] For instance, taking the

(45) Ozyilmaz, G. *J. Mol. Catal. B: Enzym.* **2009**, *56*, 231.
(46) Deng, H.-T.; Xu, Z.-K.; Dai, Z.-W.; Wu, J.; Seta, P. *Enzyme and Microbial Tech.* **2005**, *36*, 996.
(47) Yong, Y.; Bai, Y.-X.; Li, Y.-F.; Lin, L.; Cui, Y.-J.; Xia, C.-G. *Process Biochemistry* **2008**, *43*, 1179.
(48) Rahman, M. B. A.; Zaidan, U. H.; Basri, M.; Hussein, M. Z.; Rahman, R. N. Z. R. A.; Salleh, A. B. *J. Mol. Catal. B: Enzym.* **2008**, *50*, 33.
(49) Shah, S.; Sharma, S.; Gupta, M. N. *Energy Fuels* **2004**, *18*, 154.
(50) Iso, M.; Chen, B.; Eguchi, M.; Kudo, T.; Shrestha, S. *J. Mol. Catal. B: Enzymatic* **2001**, *16*, 53.
(51) Soumanou, M. M.; Bornscheuer, U. T. *Enzyme Microbial Technol.* **2003**, *33*, 97.
(52) Hernández-Matín, E.; Otero, C. *Bioresour. Technol.* **2008**, *99*, 277.
(53) Moreira, A. B. R.; Perez, V. H.; Zanin, G. M.; de Castro, H. F. *Energy Fuels* **2007**, *21*, 3689.

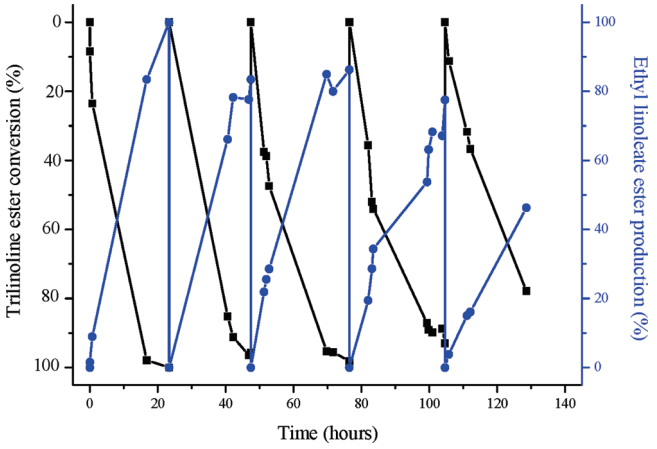

Figure 5. [C-*TL*l]@Glymo-Si(HIPE)-based trans-esterification reactions. The black line corresponds to the trilinoline ester conversion, while the blue line corresponds to the ethyl linoleiate ester production. For each experiment, the first conversions are equal to 100%; this is the reason why the catalytic performances are presented in absolute conversion performances and not using percentage relative activity.

Table 1. Catalytic Performance of Hybrid Foams

hybrid foam catalytic performance	esterification[a]	hydrolysis[a]	transesterification[b]
TON	105615	3482.61	70.8749
TOF (h^{-1})	4400.63	145.109	2.95312
enzymatic activity (μmol min^{-1} mg^{-1})	23.5	0.210	0.00483

[a] [C-*CR*l]@Glymo-Si(HIPE) catalyst. [b] [C-*TL*l]@Glymo-Si(HIPE) catalyst. The TON and TOF numbers were calculated for a single cycle; full TON and TOF can be obtained by multiplying by the number of cycles for each catalyzed reaction.

best results to date, *T. Lanuginosus* stabilized within macroporous polyglutaraldehyde-modified polymer foams achieved 90.2% within 24 h when used as a monolith, at best 97% when the monoliths were powdered, both systems at a temperature of 65 °C. Thus, our results clearly demonstrate the high efficiency of Glymo toward stabilizing *T. Lanuginosus*. Also another factor may contribute to the rather high conversion: namely, as described above for the second reaction, the inherent hydration of silica matrices, allowing optimum [C-*TL*l]@Glymo-Si(HIPE) catalytic performance (see above for stoichiometry). In fact, it is well-known that water in small amounts is an important parameter for optimization of transesterification catalytic performance when enzymes are used as catalysts.[54] We want to emphasize that in all the cycling tests dedicated to transesterification performed in this study, no water was added to the reaction medium (see Experimental Section), contrary to all previous mentioned *T. Lanuginosus*-based heterogeneous catalysts.[17,52,53] This feature is another major advantage of the [C-*TL*l]@Glymo-Si(HIPE) catalyst.

The catalytic performances of the enzyme based hybrid catalysts in all three reactions are summarized in Table 1.

The turnover number (TON) and turnover frequency (TOF) presented in Table 1 and the results reported in Figures 3-5, which correspond to absolute conversion and not to relative enzyme activity, indicate that the enzyme@Glymo-Si(HIPE) hybrid macrocellular biocatalysts presented in this study have very high conversion efficiencies in multiple catalytic cycles. For the first time, the TON and TOF numbers indicate that these materials are feasible for real industrial applications. We are currently performing uniaxial flux catalysis, in order to better optimize mass transport through the catalyst while minimizing the use of solvent. Those investigations are in progress and will be published in due time.

Conclusion

In summary, we report herein the integrative chemistry-based design of new enzyme-based macrocellular heterogeneous monolith-type biocatalysts [C-*CR*l]@Glymo-Si(HIPE) and [C-*TL*l]@Glymo-Si(HIPE), which demonstrate several favorable characteristics: high conversion percentages in multiple cycles, low steric hindrance between enzymes and substrates, minimal problems with slow diffusion rates, low cost of catalysts because of the use of crude enzymes, efficient recovery of the monolith-type catalysts allowing simple recovery and separation of end products, versatility to work either in nonaqueous or water saturated nonaqueous media, and versatility in choice of the stabilized enzymes.

With these favorable characteristics, all associated with current sustainable development issues, this study represents a significant step forward promoting robust re-emergence of enzyme-based biocatalysts for industrial applications.

Acknowledgment. This work is partially supported by the grand "Nano-cataHIPE" from the French national research agency (ANR). The authors thank Dr. Kathryn Williams of the University of Florida for her careful editing of the manuscript.

Supporting Information Available: Additional figures and information (PDF). This material is available free of charge via the Internet at http://pubs.acs.org.

(54) Antczak, M. S.; Kubiak, A.; Antczak, T.; Bielecki, S. *Renewable Energy* **2009**, *34*, 1185.